# Free-electron density effects on the exciton dynamics in coupled quantum wells

A. Hernández-Cabrera and P. Aceituno
*Departamento de Física Básica, Universidad de La Laguna, 38206 La Laguna, Tenerife, Spain*
(Received 16 December 1999; revised manuscript received 10 February 2000)

We have studied the alterations produced by the free-electron density on the dipole moment generated by the exciton oscillations in an asymmetric coupled quantum-well system. This physical situation is possible for the case of carrier injection, when the electron concentration is greater than the hole concentration, and free electrons and excitons coexist. Excitons are directly created by hole-assisted electron resonant tunneling, where doped layers supply electrons and holes. Many-body interaction and elastic scattering strongly influence the coherent dynamics of excitons, leading to time-dependent modifications of the resonant energy levels and of the level-splitting energies. As a consequence, nonperiodic charge oscillations and nonlinear regimes appear for electron densities higher than $10^{10}\,\mathrm{cm}^{-2}$. Beyond electron densities of $10^{11}\,\mathrm{cm}^{-2}$ the exciton generation can be inhibited, leading to tunneling collapse.

## I. INTRODUCTION

Semiconductor quantum wells have shown many new optical and electronic properties playing a key role in many electronic devices.[1,2] Recently, GaAs/$Ga_xAl_{1-x}As$ semiconductor coupled quantum wells have been used to observe tunneling charge oscillation in solids.[3] In such an experiment, the superposition of both symmetric and antisymmetric quantum-well eigenstates in the conduction band leads to coherent tunneling between both wells, and thus to an electron-hole pair with a time-dependent separation. Then a time-varying excitonic dipole moment in the quantum-well region is obtained, allowing the emission of electromagnetic radiation at the oscillation frequency.

There is also a great interest in other related phenomena as spatially coherent quantum-well (QW) excitons, with an in-plane momentum $\mathbf{k}_{ex\|}\sim\mathbf{0}$, due to their capability of radiating in the perpendicular direction to the QW and its possible application in vertical planar microcavities. Until now, resonant optical pumping was needed to create such excitons efficiently. In a recent experiment and theory, Cao *et al.*[4] have shown the possibility of the direct creation of electrically pumped QW excitons with $\mathbf{k}_{ex\|}\sim\mathbf{0}$. In a previous paper[5] we analyzed the exciton binding energy in asymmetric coupled quantum wells (ACQW's). In the direct generation of excitons, electrons tunnel from an *n*-type material through a barrier to the left quantum well (LQW). Owing to the structure ends in a *p*-type material (Fig. 1), we assume that holes diffuse thermally into the right quantum well (RQW) and the process is assisted by the electron-hole Coulomb interaction, and a two-particle process is obtained. Then, and under resonant conditions between two adjacent wells with different widths, electrons in the excitonic state can tunnel back and forth from one well to the other. As commented before, the generated time-dependent dipole can radiate terahertz electromagnetic waves before radiative recombination. Such a dipole moment is determined by the interwell electron density imbalance. The oscillation period, $\tau_T=2\pi\hbar/\Delta_T$, is determined by the level splitting energy $\Delta_T$ for ACQW's. Here $\Delta_T=\sqrt{\Delta^2+(2T)^2}$, where $T$ is the tunneling matrix element and $\Delta$ is the splitting for uncoupled wells. The resonance ($\Delta=0$ and $\Delta_T=2T$, the minimum splitting energy) is usually achieved by applying an electric field perpendicular to DQW layers. In order to clarify the meaning of mentioned parameters, we sketched in Fig. 2 two pairs of energy levels in the vicinity of the resonances ($\Delta=0$, indicated by arrows) for free electrons and for electrons in the exitonic state, respectively. Curves correspond to an ACQW configured by a 8-nm LQW and 6-nm RQW, separated by a 3-nm barrier, and subjected to different electric fields.

The resonant photoexcitation has been widely studied, from both the theoretical[6–11] and the experimental point of view.[2,12,13] While the concentrations of the two types of carriers forming excitons are equal in photoexcitation, the case of direct created excitons is essentially different because we can deal with two very different concentrations of electrons and holes. The different doping of electrodes causes this peculiarity. We stress here that, in the usual experimental conditions, donor concentration is greater than acceptor concentration ($\sim10^{18}$ and $\sim10^{16}\,\mathrm{cm}^{-3}$, respectively).[4] The excess of injected electrons will remain in the free-electron energy level without forming excitons and interacting not only between themselves but also with electrons trapped in excitons.

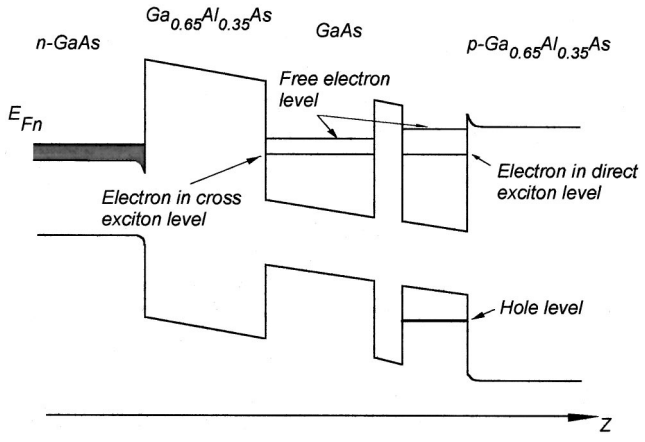


FIG. 1. Asymmetric double quantum well under the excitonic electron resonant condition in the absence of free-electron density effects.

 

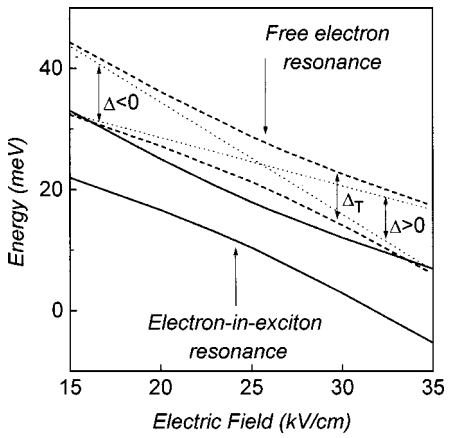


FIG. 2. Resonance position (indicated by arrows) for free electrons and for excitonic electrons as a function of an applied electric field. Solid lines: ACQW's excitonic electron levels. Dashed lines: ACQW's free-electron levels. Dotted lines: free-electron levels for decoupled QW's.

The process of direct exciton creation can be considered in two steps: First, if the Fermi level of the *n*-type material resonates with the electron level in the left well, the electron tunnels to the wide LQW forming a cross or spatially indirect (interwell) exciton with the hole diffused into the narrow RQW (see Fig. 1). Second, if the resonant condition for the electron in the excitonic state between both wells is satisfied, then the electron in the excitonic state tunnels to the RQW, forming a spatially direct (intrawell) exciton. Meanwhile, holes remain localized in the right well.

In this paper we show that, when the two constituent (electrons or holes) densities increase, many-body interactions cause both the electron in the excitonic state level and free-electron level renormalization and lead to slightly different resonant conditions for both electron species. Variation of the free-electron resonant condition with increase of the electron density is by far less noteworthy than that of excitonic electrons, but free-electron oscillations can modify excitonic electron oscillations in a determinant way. As a consequence, the charge-oscillation period also varies in a nonmonotonic manner producing even the collapse of coherent tunneling. This problem is interesting from a technological point of view because the carrier distribution could be used to control the device characteristics. It should be noticed that, in the present work, the density of carriers will not be too high ($<10^{12}\,\mathrm{cm}^{-2}$), and therefore many-body processes as phase-space occupation of the plane waves parallel to the interfaces are not relevant.[14]

The paper is organized as follows. In Sec. II we propose two coupled sets of Bloch equations to describe the dynamics of the electron in the excitonic state and free-electron densities. In Sec. III we present numerical results and discuss dynamic peculiarities of both types of electron distributions. Also, we include a brief discussion of the approximations used in calculations. Concluding remarks are presented in the last section.

## II. METHOD OF CALCULATION

In this section we analyze dissipative time-dependent excitonic processes in ACQW's, examining the dynamical evolution of excitonic electron-hole pairs as a function of the carrier density. The method of calculation is based on the matrix density formalism in the momentum representation,[10] which gives us the temporal evolution of the injected carriers. Initially, a group of electrons tunnels into the LQW. The charge, dynamically trapped by the energy-level resonance between wells, produces a reaction field that modifies the time evolution of the system.

We assume that injected electrons in the LQW, which were initially in the *n*-doped material, follow a $\delta$ distribution in time, e.g., we assume an ultrafast injection to simplify calculations. (Actually, electrons spend some time in tunneling across the left confining barrier and a Gaussian distribution may be more adequate. The analysis of the exact form of the injection and the diffusion is the subject of future work). Also, diffusion of holes from the *p*-doped material to the RQW is considered as a $\delta(t)$ function. We use the previous approximation since we are interested in knowing the evolution of densities after injection, which does not depend on any associated field, as opposed to the photoexcitation.

In order to study the dynamics of electron tunneling, we start from the quantum kinetic equation for the density operator $\hat{R}(t)$ in the momentum representation, which is obtained from the Liouville quantum equation,

$$\frac{\partial \hat{R}(t)}{\partial t}+\frac{i}{\hbar}[\hat{H},\hat{R}(t)]=0. \tag{1}$$

Here $\hat{H}$ is the many-band Hamiltonian of the ADQW, which includes the Coulomb interaction between carriers. We project Eq. (1) on the conduction band as in Ref. 8, considering the pair of tunnel-coupled states, which are described in a basis of the left ($l$) and right ($r$) QW orbitals [$\phi_l(z)$ and $\phi_r(z)$, respectively]. Such orbitals are the transverse components of electron eigenstates for the corresponding single-well cases. All the populated hole states belong to the right well, and we describe them by the set of the $r$ QW orbitals $\phi_b(z)$, where $b$ is the hole subband number. To use the orbital representation we must ensure that the injected and diffused carrier densities are small enough to neglect the deformation of the orbitals due to the screening of Coulomb interaction. This approximation is valid when the band-bending energies are small with respect to the carrier quantization energies. For the GaAs-$Ga_{0.65}Al_{0.35}As$ ADQW the approximation above can be used if carrier densities $N \leqslant 10^{12}\,\mathrm{cm}^{-2}$. The screening of the two-particle Coulomb interaction can be negligible compared with the repulsive Hartree term. It is important to mention here that the effect of the electron-hole Coulomb interaction, even if unscreened, can be canceled by other many-body processes beyond $N \approx 10^{11}\,\mathrm{cm}^{-2}$. Moreover, we neglect the transversal motion operator, which is relevant in exciton binding-energy calculations.

Following Ref. 8 the Hamiltonian of the Coulomb interaction $V_C$ is obtained from[15]

$$V_C=\frac{1}{2s}\sum_{m,n}\sum_{s,s'}\sum_{\mathbf{k},\mathbf{k}',\mathbf{q}} M_{mn}(q)a^{\dagger}_{ms\mathbf{k}+\mathbf{q}}a^{\dagger}_{ns'\mathbf{k}'-\mathbf{q}}a_{ns'\mathbf{k}'}a_{ms\mathbf{k}}. \tag{2}$$

Here $m$, $n$ indicates electron states ($l$, $r$) and hole states ($b$), $S$ is the normalization area, and $q=|\mathbf{q}|$. Coulomb matrix elements $M_{mn}(q)$ are defined as follows:

$$M_{mn}(q)=\frac{2\pi e_m e_n}{\epsilon q}\int\int dz\,dz'\,\exp(-q|z-z'|)\times|\phi_m(z)|^2|\phi_n(z')|^2, \tag{3}$$

where $e_n=e$ for $n=l,r$ and $e_n=-e$ for $n=b$, $e$ being the electronic charge and $\epsilon$ the dielectric function, which we assumed to be constant across the interfaces. In the former expressions we have made use of the same approximations as in Ref. 8. However, $M_{mn}(q)$ is quite different for free electrons and for electrons in the excitonic state. Thus, renormalization of level-splitting energies will be different for the two types of electron levels.

To obtain the one-particle contribution in the Hamiltonian $V_C$, we use the Hartree-Fock approximation that leads to the kinetic equation

$$\frac{\partial\hat{\rho}_{pt}}{\partial t}+\frac{i}{\hbar}[\hat{h}+\hat{U}_t-\hat{\Gamma}_{\mathbf{p}t},\hat{\rho}_{\mathbf{p}t}]=\hat{I}_{\mathbf{p}t}+\hat{G}_{\mathbf{p}t}, \tag{4}$$

where all terms have been described elsewhere.[8] We have introduced the collision-integral matrix $\hat{I}_{\mathbf{p}t}$ and the matrix of interband generation $\hat{G}_{\mathbf{p}t}$ as in Ref. 16. Here after we treat the collision-integral matrix in the elastic-scattering approximation. We neglect interband recombination processes because they are much slower than the scattering-induced relaxation. After integration over the electronic wave vector, we found the Bloch-equation system for the vector density $\mathbf{n}_t=(n_t^x,n_t^y,n_t^z)$ evolution

$$\frac{\partial\mathbf{n}_t}{\partial t}-[\mathbf{L}_t\times\mathbf{n}_t]=\mathbf{G}_t, \tag{5}$$

$$\frac{\partial n_t^0}{\partial t}=N\delta(t). \tag{6}$$

Here $n_t^0$ is the sheet electron density per one well, e.g., half the total density of electrons in the DQW structure; $\mathbf{G}(t)=(0,0,N\delta(t))$ is the generation term and $\mathbf{L}_t=(2T/\hbar,0,\Delta_t/\hbar)$ describes nonlinear dynamical properties of the system. Equations (5) and (6) split into two coupled Bloch systems, one for free electrons and the other for excitons. Analytical expressions are identical for both systems taking into account the different values of densities, generation terms, and level-splitting energies.

After some algebra we obtain

$$\Delta_{t,\mathrm{exc}}=\Delta+\frac{2\pi e^2}{\epsilon}\int\int dz\,dz'|z-z'|\times[|\phi_r(z')|^2-|\phi_l(z')|^2]\times\left[|\phi_l(z')|^2n_{t,\mathrm{exc}}^l+|\phi_r(z')|^2n_{t,\mathrm{exc}}^r-\sum_h|\phi_b(z)|^2n_t^b\right] \tag{7}$$

and

$$\Delta_{t,f}=\Delta+\frac{2\pi e^2}{\epsilon}\int\int dz\,dz'|z-z'|\times[|\phi_r(z')|^2-\phi_l(z')|^2]\times[|\phi_l(z')|^2n_{t,f}^l+|\phi_r(z')|^2n_{t,f}^r], \tag{8}$$

where subscripts $f$ and exc refer to free electrons and electrons in the excitonic state, respectively. It is worth mentioning that excitonic electrons not only interact among themselves and with holes but with free electrons as well. Another difference with respect to the photoexcitation case is that, in the present case, holes and electrons are located in different wells at $t=0$; $n_{t,\mathrm{exc}}^j(n_{t,f}^j)$ is the excitonic electron (free-electron) density in the $j$ well ($j=l,r$), and $n_t^b$ is the hole density in the $b$th hole subband in the right well. Under these circumstances,

$$2N_h=\sum_b n_t^b=n_{t,\mathrm{exc}}^r+n_{t,\mathrm{exc}}^l. \tag{9}$$

Here $2N_h$ is the total hole sheet density. If we denote by $2N$ the total electron density, we find

$$2N=\sum_j(n_{t,f}^j+n_{t,\mathrm{exc}}^j)=2N_f+2N_h, \tag{10}$$

where $2N_f$ is the free-electron density, and

$$n_{t,f\,(\mathrm{exc})}^z=N_{f\,(\mathrm{exc})}-n_{t,f\,(\mathrm{exc})}^r,\qquad 2n_{t,f\,(\mathrm{exc})}^z=\mathbf{n}_{t,f\,(\mathrm{exc})}^l-n_{t,f\,(\mathrm{exc})}^r, \tag{11}$$

$n_{t,\mathrm{tot}}^z=n_{t,f}^z+n_{t,\mathrm{exc}}^z$ being proportional to the total dipole moment.[17] Due to the fact that holes are located in the right well, expressions (7) and (8) become

$$\Delta_{t,\mathrm{exc}}=\Delta+\frac{4\pi e^2}{\epsilon}Z(n_{t,\mathrm{exc}}^z+N_h) \tag{12}$$

and

$$\Delta_{t,f}=\Delta+\frac{4\pi e^2}{\epsilon}Zn_{t,f}^z, \tag{13}$$

where $Z$ is the distance between the centers of the left and right wells.

Hereafter we express the $n_{t,\mathrm{exc}}^i$ densities in units of $N_h$, $n_{t,f}^i$ in units of $N_f$, and time in units of $\hbar/2T$. Also, we introduce dimensionless parameters

$$\alpha_{\mathrm{exc}}=N_h\frac{\pi e^2Z}{\epsilon T},\quad \alpha_f=N_f\frac{\pi e^2Z}{\epsilon T},\quad \kappa=\frac{\hbar}{2T\tau},\quad \beta=\frac{\Delta}{2T}. \tag{14}$$

Here $\tau$ is the relaxation time for the nondiagonal part of the density matrix.[16] Parameters $\alpha_{\mathrm{exc}}$ and $\alpha_f$ are related to the doping concentration of donors and acceptors (assuming that they are fully ionized), $\kappa$ characterizes the dissipation, and $\beta$ accounts for the coupling strength between wells and the asymmetry of the ACQW. $\beta=0$ states the resonant conditions (see Fig. 2).

Now, dimensionless Bloch equation system (5) for excitons reads

$$\dot{n}^x_{t,\mathrm{exc}}+[\beta+2\alpha_{\mathrm{exc}}(n^z_{t,\mathrm{exc}}+1)]n^y_{t,\mathrm{exc}}+\kappa n^x_{t,\mathrm{exc}}=0,$$

$$\dot{n}^y_{t,\mathrm{exc}}-[\beta+2\alpha_{\mathrm{exc}}(n^z_{t,\mathrm{exc}}+1)]n^x_{t,\mathrm{exc}}+\kappa n^y_{t,\mathrm{exc}}+n^z_{t,\mathrm{exc}}=0, \tag{15}$$

$$\dot{n}^z_{t,\mathrm{exc}}-n^y_{t,\mathrm{exc}}=0,$$

where $\dot{n}^i_t=dn^i_t/dt$. The previous system is coupled to the corresponding system for free electrons:

$$\dot{n}^x_{t,f}+(\beta+2\alpha_f n^z_{t,f})n^y_{t,f}+\kappa n^x_{t,f}=0,$$

$$\dot{n}^y_{t,f}-(\beta+2\alpha_f n^z_{t,f})n^x_{t,f}+\kappa n^y_{t,f}+n^z_{t,f}=0, \tag{16}$$

$$\dot{n}^z_{t,f}-n^y_{t,f}=0,$$

with the initial conditions $n^z_{t,i}=1$ and $\dot{n}^z_{t,i}=0$ at $t=0$. We can see from expressions (15) and (16) the distinct resonant positions for excitonic electrons and for free electrons. Solving both systems jointly we get $n^z_{t,\mathrm{tot}}$, which is proportional to the total dipole moment, as we have stated above.

### III. RESULTS AND DISCUSSION

In this work we consider an ACQW potential (Fig. 1), with a distance between the centers of the wells $Z\approx 10$ nm. For typical experimental conditions, $2T\approx 5$ meV and $\epsilon=12$, we obtain that $\alpha_i=1$ corresponds to a sheet density $N_i\approx 5\times 10^{10}\,\mathrm{cm}^{-2}$, and $\kappa=0.1$ corresponds to a relaxation time $\tau\approx 1.3$ ps.

To analyze the response of the electron system as function of time, we perform numerically the coupled systems (15) and (16) through the Runge-Kutta method. We will focus our attention on the most interesting results corresponding to the cases in which the concentrations of injected electrons are higher than thermally diffused hole concentrations. At first we have studied the influence of the free-electron concentration on the oscillatory regime of excitons. For this purpose we used a fixed hole density of $N_h\approx 10^{10}\,\mathrm{cm}^{-2}$ ($\alpha_{\mathrm{exc}}=0.2$), varying the injected electrons in a range between $N=N_h$ and $N=10N_h$ (there are no remarkable differences for lower $N_h$ values except a very low increase in the oscillation period, upon making it $N_h$). Figure 3(a) shows the time evolution of $n^z_{t,\mathrm{tot}}$ for $(\alpha_{\mathrm{exc}},\beta)=(0.2,-0.4)$ and $\kappa=0.05$. The factor $(\beta+2\alpha_{\mathrm{exc}})$ is equal to $\Delta_{t,\mathrm{exc}}/2T$ at $n^z_{t,\mathrm{exc}}=0$ and $\beta=\Delta_{t,f}/2T$ at $n^z_{t,f}=0$, and correspond to the level-splitting energies at $t\to\infty$. $\beta=-2\alpha_{\mathrm{exc}}$ gives us maximum excitonic electron oscillation amplitude for each density.[18] Panel 1 represents the behavior for the two excitonic electron levels close to their resonance. As soon as the free-electron density increases, the renormalization of energy levels slightly sets excitonic electron levels apart from resonance and places free-electron levels near resonance. Moreover, the excitonic electron level approaches the free-electron level. As a consequence quantum beats appear (panel 2). From a physical point of view, the higher density of injected electrons produces a relative widening of the excitonic electron level splitting and a relative narrowing of the free-electron level splitting. Then the free-electron oscillation amplitude dominates dipole moment for $N\sim 6\times 10^{10}\,\mathrm{cm}^{-2}$ (panel 3). Finally, the positive part of the Hartree potential cancels the attractive Coulomb interaction. As a consequence, excitons no longer exist, giving rise to a dense gas of free electrons, and a ''chaotic'' behavior occurs (panel 4). Such a situation is delayed for higher hole densities ($\alpha_{\mathrm{exc}}=1$). Panel 1 of Fig. 3(b) presents the appearance of the nonlinear regime for excitons, and quantum beats remain even for injected densities beyond $N\sim 10^{11}\,\mathrm{cm}^{-2}$.

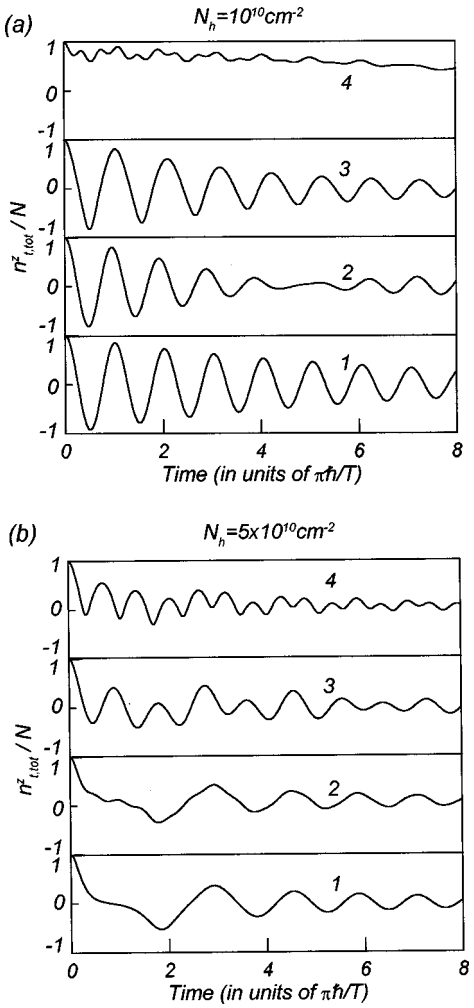


FIG. 3. Time evolution of normalized dipole moment for a fixed excitonic electron (or hole) sheet density $N_h$ close to resonance and for different values of $(\alpha_i,\beta)$. (a) $N_h=10^{10}\,\mathrm{cm}^{-2}$, $\alpha_{\mathrm{exc}}=0.2$, and $\beta=-0.4$. Panel 1: $\alpha_f=0$; panel 2: $\alpha_f=0.2$; panel 3: $\alpha_f=1$; panel 4: $\alpha_f=1.8$. (b) $N_h=5\times 10^{10}\,\mathrm{cm}^{-2}$, $\alpha_{\mathrm{exc}}=1$, and $\beta=-2$. Panel 1: $\alpha_f=0$; panel 2: $\alpha_f=0.2$; panel 3: $\alpha_f=1$; panel 4: $\alpha_f=1.8$.

Figures 4(a) and 4(b) include a parallel analysis for a fixed density of injected electrons. For (a), $\alpha_{\mathrm{tot}}=1$, the sheet density $N_h$ of diffused holes varying from 0 to $4\times 10^{10}\,\mathrm{cm}^{-2}$; for (b), $\alpha_{\mathrm{tot}}=2$, with $N_h$ ranging from 0 to $8\times 10^{10}\,\mathrm{cm}^{-2}$. Panel 1 of Fig. 4(a) shows the situation in which only free electrons are present. Once holes have been introduced into the RQW, the density of free electrons is reduced, and the corresponding relative energy splitting increases. It should be noted that energy splitting is a time-dependent function due to its dependence on $n^z_{t,f}$. The relative increase of the energy splitting refers to its value for $N_h(N_f)\to 0$. Once the hole density (excitonic electron density) exceeds the free-electron density, anharmonic oscillations occur (panels 3 and 4). Figure 4(b) shows a similar behavior of the dipole moment (for a fixed $N=10^{11}\,\mathrm{cm}^{-2}$) as

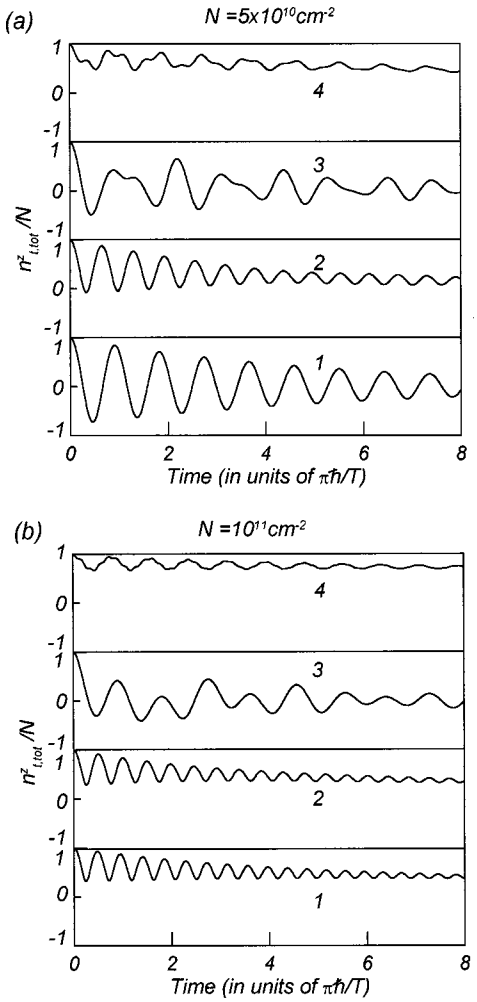


FIG. 4. The same as Fig. 3 for fixed injected-electron sheet density $N$ and for $\beta=-2\alpha_{\rm exc}$. (a) $N=5\times10^{10}\,{\rm cm}^{-2}$. Panel 1: $\alpha_{\rm exc}=0$, $\alpha_f=1$. Panel 2: $\alpha_{\rm exc}=0.2$, $\alpha_f=0.8$. Panel 3: $\alpha_{\rm exc}=0.5$, $\alpha_f=0.5$. Panel 4: $\alpha_{\rm exc}=0.8$, $\alpha_f=0.2$. (b) $N=10^{11}\,{\rm cm}^{-2}$. Panel 1: $\alpha_{\rm exc}=0$, $\alpha_f=2$. Panel 2: $\alpha_{\rm exc}=0.4$, $\alpha_f=1.6$. Panel 3: $\alpha_{\rm exc}=1$, $\alpha_f=1$. Panel 4: $\alpha_{\rm exc}=1.6$, $\alpha_f=0.4$.

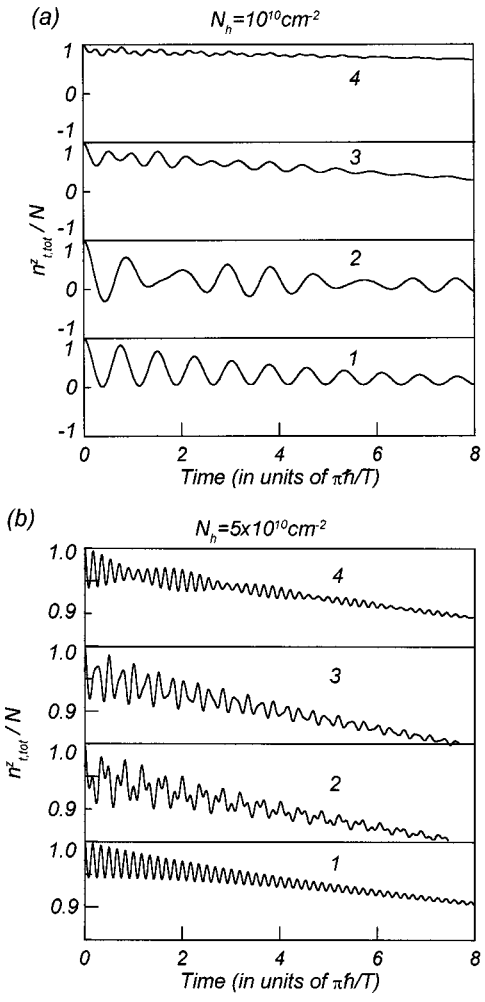


FIG. 5. The same as Fig. 3 for a fixed hole density and for excitonic electron far from resonant conditions. (a) $N_h=10^{10}\,{\rm cm}^{-2}$ and $\beta=0.2$. (b) $N_h=5\times10^{10}\,{\rm cm}^{-2}$ and $\beta=1$. $\alpha_i$ values for panels 1–4 are the same as for Fig. 2.

in Fig. 4(a). Of course, higher density produces a decrease of the $n^z_{t,i}$ oscillation amplitude due to the electron-electron interaction and changes in resonant conditions. We use a $\kappa=0.05$ value in calculations.

The set of Figs. 5 and 6 represents the total dipole moment for the same densities of holes and electrons than in Figs. 3 and 4, but far from the excitonic electron resonant condition ($\alpha_{\rm exc}=\beta$ in Figs. 5 and 6). The most interesting situations occur for $N_h\approx5\times10^{10}\,{\rm cm}^{-2}$ [Fig. 5(b)]. After a transient anharmonic regime quantum beats appear for $N\approx1.4\times10^{11}\,{\rm cm}^{-2}$, and free-electron oscillations are modulated for the very low excitonic electron oscillations because free electrons are closer to their resonances than excitons.

A general feature that we have mentioned above is the relation of anharmonic responses with the electronic concentrations, which can be expressed in terms of the charge density.[19] In the absence of dissipation and for electronic densities lower than $2\times10^{10}\,{\rm cm}^{-2}$, the harmonic oscillatory behavior persists unaltered during a long time due to the very low influence of many-body contributions and to the separation far from the resonance for free-electron levels. Beyond the last density the shift of the resonance causes a partially transmitted electronic charge across the central barrier. The magnitude of the remaining charge depends on the carrier concentration. Then initial amplitude of oscillations depends on carrier density as Figs. 3–6 show. Of course, the oscillation amplitude also decreases with time due to dissipative damping. This situation can be explained using the following arguments: the space-charge potential is a consequence of the difference between the spatial distribution of electrons and holes. In our proposed system, electrons are not localized but holes are confined within the right well layer. The space-charge potential is repulsive for the localized holes and attractive for electrons. To obtain an accurate carrier distribution one must include the Hartree potential self-consistently. As a consequence, at low carrier concentrations, the electron-hole interaction dominates over electron-electron and hole-hole repulsion. This fact was shown in Ref. 5, where only the electron-hole Coulomb interaction was included. An increase in the number of carriers helps in increasing the repulsive part of the Hartree potential to equal the Coulomb interaction. From this point the oscillation period strongly decreases.[19] These results agree fairly well with those of Raichev[8] about photoexcited carriers. When the

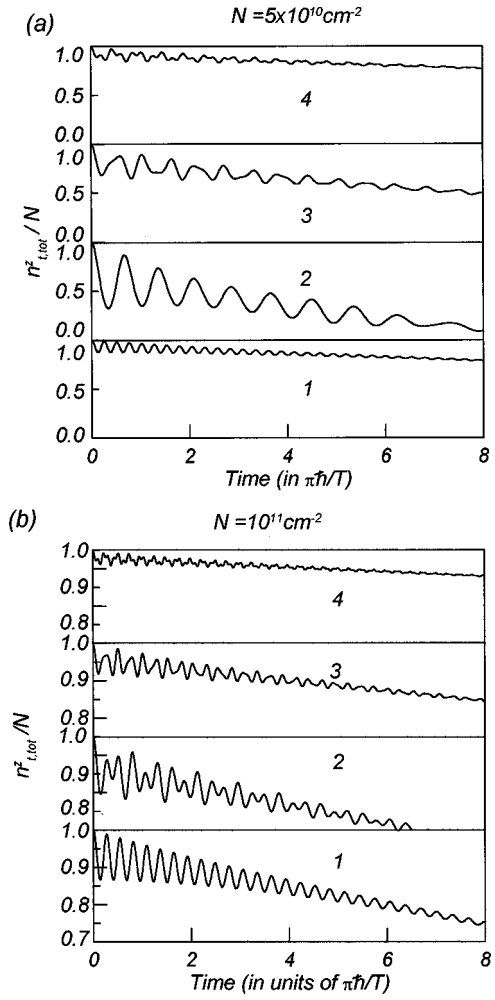


FIG. 6. The same as Fig. 4 for fixed injected-electron sheet density $N$ and $\beta=\alpha_{\rm exc}$ (a) $N=5\times10^{10}\,{\rm cm}^{-2}$. Panel 1: $\alpha_{\rm exc}=0$, $\alpha_f=1$. Panel 2: $\alpha_{\rm exc}=0.2$, $\alpha_f=0.8$. Panel 3: $\alpha_{\rm exc}=0.5$, $\alpha_f=0.5$ Panel 4: $\alpha_{\rm exc}=0.8$, $\alpha_f=0.2$. (b) $N=10^{11}\,{\rm cm}^{-2}$. Panel 1: $\alpha_{\rm exc}=0$, $\alpha_f=2$. Panel 2: $\alpha_{\rm exc}=0.4$, $\alpha_f=1.6$. Panel 3: $\alpha_{\rm exc}=1$, $\alpha_f=1$. Panel 4: $\alpha_{\rm exc}=1.6$, $\alpha_f=0.4$.

Coulomb interaction is absolutely canceled, excitonic electron levels and free-electron levels coincide and excitons disappear.

Some comments about approximations used in calculations are now given. We assumed an ultrafast injection and diffusion into the wells, such that the duration of such processes is shorter than the period of the coherent oscillations. Since the interwell separation $Z$ ($\sim$10nm) is typically of the order of the exciton Bohr radius $a_B$, we neglected the exchange contribution in comparison with the direct Coulomb contribution, due to the small value of $\hbar/\sqrt{m\bar{\varepsilon}}Z$, where $\bar{\varepsilon}$ is the mean energy of the injected electrons. Also, we assumed that $\bar{\varepsilon}$ is large with respect to the effective level-splitting energies for the DQW.

We would like to mention here that, at densities much less than that required to produce unbinding, an exciton can bind with a second excess electron to form a negatively charged exciton (a trion, $X^-$).[20] We did not consider in this work the possibility of forming trions because of the electric-field-induced ionization of these complexes. A modest electric field ($\sim$ 10 kV/cm) applied normal to QW's causes a sharp reduction in the second electron binding energy of $X^-$.[21] The electric field required to achieve the electron resonance in our proposed structure is about 25 kV/cm. We expected that the formation of such complexes should be quenched at this electric field.

## IV. CONCLUSIONS

We have studied the free-electron density effects on the time evolution of direct created excitons by means of two coupled Bloch systems, obtained from the Liouville quantum equation. The excitonic dynamics is basically determined by carrier concentrations and the dissipation even for narrow-gap materials. Our results show that, for electron densities higher than $10^{10}\,{\rm cm}^{-2}$, the repulsive part of the Hartree potential tends to equal the electron-hole Coulomb potential and the oscillation period decreases. When the repulsive part of the Hartree potential cancels electron-hole Coulomb interaction, excitons no longer exist. Also, we have found a very rich variety of responses, from modulation and quantum beats to an anharmonic regime, as a consequence of the different densities of the two kinds of electron levels. Densities mainly affect level-splitting energies and resonances (coupling strength). Electron oscillations together with the confined hole will lead to a nonlinear coherent electromagnetic radiation emerging from the semiconductor ACQW, after electrical injection. Taking into account that the mean life for an electron-hole pair in GaAs is longer than 100 ps, an experimental observation of such a process can be possible. Other quantities, such as current densities (which are directly translated into terahertz radiation), can be straightforwardly calculated with this method as well.

It should be noticed that, unfortunately, only photoexcitation experiments for ACQW's are available. In such experiments, the main effect of the photoexcited carrier density is a reduction of both the oscillation period and amplitude.[10] In practice, the electron density is low ($\lesssim10^{11}\,{\rm cm}^{-2}$), even in electronic injection, to produce considerable nonlinear effects. Then, we studied effects of the Coulomb interaction only in the first order of perturbation theory, neglecting fluctuations of the electron density. Such fluctuations lead to the dephasing of the coherent oscillations. This dephasing effect increases with the excitation density $\alpha$. Then, we restricted ourselves to moderately low values of the excitation density ($\alpha\leqslant2$).

It can be concluded that, though the most adequate densities for practical purposes in our structure (for achieving an appreciable oscillation amplitude and a constant period) are included between $10^9$ and $10^{10}\,{\rm cm}^{-2}$, some density-dependent processes such as modulation of radiation, quantum beats, and nonlinear responses promise interesting technical applications in commutation and communications. Therefore, the detailed study of high-density peculiarities deserves special attention.

## ACKNOWLEDGMENT

This work has been supported in part by Gobierno Autónomo de Canarias: Consejería de Educación, Cultura y Deportes.

[1] L. Esaki, IEEE J. Quantum Electron. **QE-22**, 1611 (1986).
[2] M. Abe, T. Mimura, K. Nishiuchi, A. Shibatomi, and M. Kobayashi, IEEE J. Quantum Electron. **QE-22**, 1870 (1986).
[3] H. G. Roskos, M. C. Nuss, J. Shah, K. Leo, D. A. B. Miller, A. M. Fox, S. Schmitt-Rink, and K. Köhler, Phys. Rev. Lett. **68**, 2216 (1992); P. C. M. Planken, M. C. Nuss, I. Brener, K. W. Goosen, M. S. C. Luo, S. L. Chuang, and L. Pfeiffer, *ibid.* **69**, 3800 (1992).
[4] H. Cao, G. Klimovitch, G. Björk, and Y. Yamamoto, Phys. Rev. B **52**, 12 184 (1995); Phys. Rev. Lett. **75**, 1146 (1995).
[5] P. Aceituno, H. Cruz, and A. Hernández-Cabrera, Phys. Rev. B **54**, 17 677 (1996).
[6] P. C. M. Planken, I. Brener, M. C. Nuss, M. S. C. Luo, and S. L. Chuang, Phys. Rev. B **48**, 4903 (1993); M. S. C. Luo, S. L. Chuang, P. C. M. Planken, I. Brener, and M. C. Nuss, *ibid.* **48**, 11 043 (1993).
[7] F. T. Vasko and O. E. Raichev, Phys. Rev. B **51**, 16 965 (1995); O. E. Raichev, F. T. Vasko, A. Hernández-Cabrera, and P. Aceituno, J. Appl. Phys. **80**, 5106 (1996).
[8] O. E. Raichev, Phys. Rev. B **51**, 17 713 (1995).
[9] E. Binder, T. Kuhn, and G. Mahler, Phys. Rev. B **50**, 18 319 (1994).
[10] F. Rossi, T. Meier, P. Thomas, S. W. Koch, P. E. Selbmann, and E. Molinari, Phys. Rev. B **51**, 16 943 (1995); F. Rossi, Semicond. Sci. Technol. **13**, 147 (1998).
[11] W. Pötz, M. Ziger, and P. Kocevar, Phys. Rev. B **52**, 1959 (1995).
[12] M. C. Nuss, P. C. M. Planken, I. Brener, H. G. Roskos, M. S. C. Luo, and S. L. Chuang, Appl. Phys. B: Lasers Opt. **58**, 249 (1994).
[13] V. Z. Tronciu and A. H. Rotaru, Phys. Status Solidi B **212**, 383 (1999); N. Sekine, K. Hirakawa, and Y. Arakawa, Jpn. J. Appl. Phys., Part 1 **37**, 1643 (1998); N. Garro, M. J. Snelling, S. P. Kennedy, R. T. Phillips, and K. H. Ploog, J. Phys.: Condens. Matter **11**, 6061 (1999).
[14] B. Olejniková, Superlattices Microstruct. **14**, 215 (1993).
[15] C. Kittel, *Quantum Theory of Solids* (Wiley, New York, 1963).
[16] F. T. Vasko and O. E. Raichev, Zh. Eksp. Teor. Fiz. **108**, 21 033 (1995) [Sov. Phys. JETP **81**, 1146 (1995)].
[17] O. E. Raichev, F. T. Vasko, A. Hernández-Cabrera, and P. Aceituno, Phys. Rev. B **56**, 4802 (1997).
[18] J. M. Hernández, A. Hernández-Cabrera, and P. Aceituno (unpublished).
[19] A. Hernández-Cabrera, Physica E (Amsterdam) **4**, 65 (1999).
[20] K. Kheng, R. T. Cox, Y. Merle d'Aubigné, F. Bassani, K. Saminadayar, and S. Tatarenko, Phys. Rev. Lett. **71**, 1752 (1993); H. Buhmann, L. Mansouri, J. Wang, P. H. Beton, N. Mori, L. Eaves, M. Henini, and M. Potemski, Phys. Rev. B **51**, 7969 (1995); G. Finkelstein, H. Shtrikman, and I. Bar-Joseph, *ibid.* **53**, R1709 (1996); A. J. Shields, J. L. Osborne, D. M. Whittaker, M. Y. Simmons, M. Pepper, and D. A. Ritchie, *ibid.* **55**, 1318 (1997); D. B. Turchinovich, V. P. Kochereshko, D. R. Yakovlev, W. Ossa, G. Landwehr, T. Wojtowicz, G. Karczweski, and J. Kossut, Fiz. Tverd. Tela **40**, 813 (1998) [Phys. Solid State **40**, 747 (1998)].
[21] A. J. Shields, F. M. Bolton, M. Y. Simmons, M. Pepper, and D. A. Ritchie, Phys. Rev. B **55**, R1970 (1997).